

submitted for publication in the
International Journal of Thermophysics

**Anisotropic Thermal Diffusivity Measurements in Deforming Polymers
and the Stress-Thermal Rule¹**

D.C. Venerus^{2,3}, J.D. Schieber², H. Iddir², J. Guzmán², and A. Broerman²

¹ Paper presented at the Fourteenth Symposium on Thermophysical Properties, June 25-30, 2000, Boulder, Colorado, U.S.A.

² Department of Chemical Engineering and Center of Excellence in Polymer Science and Engineering, Illinois Institute of Technology, Chicago, Illinois 60616 U.S.A.

³ To whom correspondence should be addressed.

ABSTRACT

In recent years, both experimental and theoretical research on energy transport in deforming polymeric materials have increased. Theoretical results indicate that the thermal conductivity in such systems is anisotropic, and support, analogous to the well-known stress-optic rule, the validity of a stress-thermal rule where the thermal conductivity and stress tensors are linearly related. In this study we have developed a method to measure the thermal diffusivity in deforming polymers. The method is based on an optical technique known as Forced Rayleigh Scattering. This sensitive and non-invasive technique is shown to be capable of quantitative measurements of anisotropic thermal diffusivity in both static and dynamic (relaxing) polymers subjected to deformations. Results have been obtained for a polymer melt in step-shear strain flows and a cross-linked elastomer in uniaxial extension. Thermal diffusivity data are complemented by measurements of stress and birefringence so that evaluations of the stress-optic and stress-thermal rules can be made. We find that the thermal diffusivity is enhanced in the flow (or stretch) direction compared to the equilibrium value and that the stress-thermal rule is valid for the modest deformations achieved in this study.

KEYWORDS: anisotropic, thermal conduction, forced Rayleigh scattering

1. INTRODUCTION

Polymeric materials are, because of their high viscosity and low thermal conductivity, often subject to large temperature gradients during processing. Since mechanical properties such as viscosity and relaxation time are strongly temperature dependent, accurate knowledge of the thermal properties of polymers is essential for the development of accurate process models. Therefore, the study of thermal transport in polymers has been the subject of intense research in recent years [1].

Recent theoretical work has postulated the existence of anisotropic thermal conduction in polymeric liquids undergoing deformation [2-4]. Experimental studies of heat conduction in crosslinked polymers have revealed an anisotropic thermal conductivity under elongational stretch [5,6]. It would seem reasonable that thermal conductivity would be anisotropic in deforming polymeric systems. Indeed, anisotropy in mechanical and optical properties resulting from flow-induced orientation of polymer chains can be rather pronounced. In such cases, Fourier's Law is expressed in terms of a thermal conductivity *tensor* \mathbf{k} as follows:

$$\mathbf{q} = -\mathbf{k}\nabla T \tag{1}$$

where \mathbf{q} is the energy flux and T the temperature.

Measurements of thermal conductivity (or diffusivity) in flowing polymer liquids are somewhat scarce, however, and data that have been published are somewhat ambiguous. For example, results for steady shear flow of molten polymers indicate that the thermal conductivity perpendicular to the flow direction first increased and then decreased with increasing shear rate for one polymer while showing the opposite trend for a different polymer [7].

The widely accepted stress-optic rule [8], which relates the refractive index tensor \mathbf{n} to the extra stress tensor $\mathbf{\tau}$, can be written as

$$\mathbf{n} - \frac{1}{3}\text{tr}(\mathbf{n}) = C\boldsymbol{\tau} \quad (2)$$

where C is the stress-optic coefficient. The stress-optic coefficient has been determined for a large number of polymers and found to be relatively insensitive to strain, strain rate, temperature and molecular weight in shear flows and moderate elongational deformations [8].

The existence of a stress-*thermal* rule was first suggested by van den Brule [2] using arguments based on a network theory model for polymer chains. In terms of the thermal diffusivity tensor $\mathbf{D} = k/\rho C_p$, where ρ is mass density and C_p is specific heat capacity, the stress-thermal rule is

$$\left(\mathbf{D} - \frac{1}{3}\text{tr}(\mathbf{D}) \right) \frac{1}{D_{\text{eq}}} = C_t \boldsymbol{\tau} \quad (3)$$

where D_{eq} is the equilibrium thermal diffusivity, and C_t is the *stress-thermal coefficient*.

In this study we present quantitative measurements of deformation-induced anisotropic conduction for two systems: a polymer melt subjected to simple shear, and a cross-linked rubber subjected to uniaxial elongation. These data are complimented by measurements of stress and birefringence so that evaluations of the stress-optic and stress-thermal rules can be made.

2. EXPERIMENTAL CONSIDERATIONS

In this work, we have adapted the optical technique known as Forced Rayleigh Scattering (FRS) to measure thermal diffusivity in deforming polymers. FRS has been used previously to study diffusive transport in a wide range of systems [9] including measurements of thermal diffusion in polymer solutions [10] and anisotropic thermal diffusivity in oriented polymer solids [11]. Details of the FRS setup in our laboratory can be found elsewhere, which has been used for quiescent

polymer melts [12], a sheared polymer melt [13], and a stretched silicone rubber [14].

The FRS technique for thermal diffusivity measurement uses crossed beams of a writing laser (Ar^+) to induce a fringe pattern with period Λ in the sample, which contains dye that absorbs the impinging light. By radiationless decay, the dye then creates a temperature field T having a sinusoidal spatial modulation $\delta T = T - T_b$, where T_b is the bulk temperature of the sample. As a consequence of the temperature dependence of the refractive index, an optical (phase) grating is created in the sample. Because the grating period Λ is much smaller than the spot size of the writing laser, the dynamics of the grating temperature field δT can be decoupled from the bulk sample temperature T_b . Furthermore, if conditions for the plane grating approximation [9,12] are satisfied, δT is governed by the following:

$$\frac{\partial \delta T}{\partial t} = D_{ii} \frac{\partial^2 \delta T}{\partial x_i^2} + \frac{KI}{\rho C_p} \cos\left(\frac{2\pi x_i}{\Lambda}\right) \quad (4)$$

where K is the absorptivity of the sample at the writing laser wavelength (515 nm) and I is the time-dependent intensity of the writing laser. In Eq. (4), the grating is oriented either parallel ($i=1$) or perpendicular ($i=3$) to the direction of flow or stretch; it does not contain any convective flow terms, since the temperature grating is created and decays only after the deformation is imposed. It is assumed in Eq. (4) that the temperature dependence of k_{ii} can be neglected, which is justified since δT is typically of the order 0.01°C .

Following a pulse from the writing laser ($t > t_p$), when $I = 0$, the grating temperature decays according to

$$\delta T(t) \propto e^{-t/\tau_g} \quad (5)$$

where the grating relaxation time τ_g is given by

$$\tau_g = \frac{\Lambda^2}{4\pi^2 D_{ii}} \quad (6)$$

and where $D_{ii} = k_{ii}/\rho C_p$ is the thermal diffusivity in the i -direction.

Dynamics of the grating are probed by a low-power HeNe laser ($\lambda_{\text{HeNe}} = 633 \text{ nm}$). When introduced at the Bragg angle, the reading laser beam is diffracted by the thermal grating with a diffraction efficiency proportional to $(\delta T)^2$. A photodetector detects the first-order diffracted beam, which decays according to Eq. (5), along with coherently and incoherently scattered light producing a voltage that decays according to

$$V(t) = \bar{A}e^{-2t/\tau_g} + \bar{B}e^{-t/\tau_g} + \bar{C} \quad (7)$$

where A , B and C are constants. C is measured at long times following the pulse while A , B and τ_g were fit to the data by a Levenberg-Marquardt method described elsewhere [12].

Measurements of birefringence $\Delta n_{13} = n_{11} - n_{33}$ were made using the HeNe laser and an optical train consisting of a sample of thickness d between crossed polarizers oriented at $\pm \pi/4$ with respect to the direction of flow/stretch. The ratio of the transmitted to incident intensity of the laser is related to the retardance δ [8], which is related to the birefringence as follows

$$\delta = \frac{\pi d \Delta n_{13}}{\lambda_{\text{HeNe}}} \quad (9)$$

Two polymer systems were examined in this study. One was a broad molecular weight distribution poly-isobutylene melt having a weight-average molecular weight of approximately 85,000. The mean relaxation time τ_p of this material at 25°C is approximately 45 s. The second polymer system was a cross-linked vinyl methyl poly-siloxane. A dye known as

quinizarin, which absorbs at a wavelength of 515 nm but is nearly transparent at 633 nm, was uniformly dispersed within the samples. Details of the sample preparation methods can be found elsewhere [12,14].

Shear deformations were imposed on the polymer melt in a parallel plate flow device. One plate was stationary while the other was driven by several stiff springs. Each plate had a glass window that formed an optical path through the sample after the deformation had been imposed. Shear strains Υ of four and eight were imposed in less than 75 ms making them effectively ‘step’ deformations. Simple elongational deformations were imposed on the silicone rubber by displacing the clamped ends and measuring the distance L between parallel lines marked on the sample that were separated by a distance L_0 on the undeformed sample. The elongation ratio is given by $\lambda = L/L_0$, and was limited to values of approximately two because sample failure occurred at larger strains.

3. RESULTS AND DISCUSSION

A sample waveform for the polymer melt at a time of 150 msec following a step shear strain $\Upsilon = 8$ is shown in Fig. 1, which shows the voltage from the photodetector both during and following the pulse of the writing laser. However, only the voltage following the pulse is fit by Eq. (7). The inset in Fig. 1 is a histogram of the residuals $V(t) - V_{\text{fit}}$. The Gaussian distribution of the residuals confirms the validity of Eq. (7); it also verifies our assumption of constant thermal diffusivity during the decay of a grating, which one would expect since $\tau_g \ll \tau_p$ [13].

As noted earlier, Eq. (4) does not include the effects of flow is because the velocity v is zero during the formation and decay of the thermal grating. The generalization of Eq. (4) to include convective flow effects is not trivial, but would seem necessary unless the grating relaxation τ_g is much smaller than the grating period Λ divided by the magnitude of the velocity: $\tau_g \ll \Lambda/v$.

Otherwise, bulk flow would smear the grating resulting in a larger grating decay rate (smaller τ_g and larger D_{ii}) than in the absence of flow. In such cases, it is unlikely the decay of $V(t)$ could be fit to Eq. (7). In a previous study where FRS was used to measure thermal diffusivity in the constant rate flow of a polymer melt through a slit [15], relaxation of the grating was *assumed* to be governed by $V(t) \propto \exp(-2t/\tau_g)$, even though convective flow was affecting the grating decay dynamics. In other words, no curve fitting procedure was used; τ_g was determined by the condition: $V(\tau_g/2+t_p)/V(t_p) = 1/e$ [15].

According to Eq. (6), a plot of $1/\tau_g$ versus $4\pi^2/\lambda^2$ should be linear with a slope equal to the thermal diffusivity D_{ii} . If D_{ii} is a function of time following the step strain, but constant during the decay of a grating, i.e., $\tau_g \ll \tau_p$, then isochronal values of τ_g over a range of λ can be used to make this check. Figure 2 shows such a plot for several times following the imposition of the shear strain ($\Upsilon = 8$) with the grating oriented in the flow direction. Each data point represents a result from a single waveform (of the kind shown in Fig. 1) at a given time following the imposition of the strain. The different solid lines were fit to points corresponding to different times (symbols) following the step strain. The good correlation of the data points with the straight lines is consistent with the use of Eq. (4), and confirms the validity of Fourier's Law generalized to allow anisotropy, Eq. (1). The slopes of the solid lines correspond to thermal diffusivity measured in the flow direction, D_{11} , at different times. From Figure 2 it also appears that D_{11} approaches the equilibrium value D_{eq} ($= 0.66 \pm 0.03 \times 10^{-3} \text{ cm}^2/\text{s}$) with increasing time.

Values of thermal diffusivity in the flow direction D_{11} (obtained as shown in Fig. 2) and the neutral direction D_{33} (obtained in the same manner), normalized by D_{eq} , are shown in Fig. 3 as functions of time following the imposition of step strains $\Upsilon = 4$ and 8. In the flow direction, the thermal diffusivity is increased above the equilibrium value by approximately 20% (for $\Upsilon=8$)

immediately following the step strain whereas a decrease of approximately five percent is observed for the neutral direction. For all the data shown, the thermal diffusivity appears to be relaxing to its equilibrium value D_{eq} (indicated by dashed line).

In order to examine the connection between flow-induced chain segment orientation and anisotropic thermal diffusivity, we plot the normalized thermal diffusivity difference $(D_{11} - D_{33})/D_{eq}$ versus birefringence Δn_{13} in Figure 4 for $\Upsilon = 4$ and 8. The data in this figure are consistent with the straight line indicating that $D_{11} - D_{33}$ is proportional to Δn_{13} , which suggests flow-induced orientation of polymer chain segments is responsible for anisotropy in both optical and thermal transport properties. The data in Figure 4 support a linear combination of Eqs. (2) and (3), or a thermal-optic rule; the slope of the line in this figure corresponds to the ratio C_1/C .

The FRS procedures described above were also applied to cross-linked siloxane samples subjected to uniaxial elongations [14]. Waveforms and fits of Eq. (7) were qualitatively similar to that shown in Figure 1 for the polymer melt. Also, the validity of Eq. (6) was examined by systematic variation of the grating period. Results from this procedure were similar to those shown in Figure 2 for the polymer melt, where time following the step strain is replaced by the elongation ratio λ . Figure 5 shows the thermal diffusivities normalized by D_{eq} ($= 1.08 \pm 0.02 \times 10^{-3} \text{ cm}^2/\text{s}$) in both the stretch and contraction directions versus elongation ratio. Thermal diffusivity increases/decreases in the stretch/contraction direction as λ is increased. In Figure 6, the normalized thermal diffusivity difference $D_{11} - D_{33}$ is plotted versus tensile stress $\sigma = \tau_{11} - \tau_{33}$. It appears that within the uncertainty of the experimental data a linear relationship is observed. These data appear to be the first direct evidence that *support the validity of a stress-thermal law*, Eq. (3), where the stress and thermal conductivity tensors are linearly related [2].

The results presented above clearly support the stress thermal rule, Eq. (3), and,

consequently, it is possible to estimate values for the stress-thermal coefficient, C_t for the two polymer systems. For the poly-isobutylene melt, the data in Figure 4 provide a value for $C_t/C = 75$; using the reported value [8] for the stress-optic coefficient C , we find $C_t = 1.6 \times 10^7 \text{ Pa}^{-1}$. For the cross-linked poly-siloxane, the data in Figure 6 can be used directly to obtain $C_t = 1.3 \times 10^7 \text{ Pa}^{-1}$, which is remarkably close to the value for the poly-isobutylene melt. These results are summarized in Table 1, which also includes the maximum values for the principal stretch λ_{max} . For shear flow the principal stretch is calculated by the following: $\lambda_{\text{max}} = (\gamma + \sqrt{\gamma^2 + 4})/2$. The results in Table 1 are the first experimental tests of the stress-thermal rule. If, as noted by van den Brule [2], the stress-thermal rule were found to enjoy some degree of generality, similar to the stress-optic rule, for example, then future developments in the study of non-isothermal deformations of polymeric materials would be greatly facilitated.

4. CONCLUSIONS

Deformation-induced anisotropic thermal conductivity has been studied in two polymer systems using a sensitive and non-invasive optical technique known as Forced Rayleigh Scattering. For the polymer melt subject to shear deformations, measured thermal diffusivities in the flow/neutral direction were found to increase/decrease by up to 20%/5% relative to the equilibrium value. In the case of the cross-linked rubber subject to uniaxial elongation, anisotropies of roughly 20% relative to the equilibrium value were observed. These data, in conjunction with optical and mechanical data, support a recently proposed stress-thermal rule.

ACKNOWLEDGMENTS

The authors are grateful to the National Science Foundation (CTS-9509754) and the Amoco Foundation for support of this study.

REFERENCES

- [1] M. Dressler, B.J. Edwards, and H.C. Öttinger, *Rheol. Acta* **38**: 117 (1999).
- [2] B.H.A.A. van den Brule, *Rheol. Acta* **28**: 257 (1989).
- [3] C.F. Curtiss and R.B. Bird, *Adv. Polym. Sci.* **125**: 1 (1996); R.B. Bird, C.F. Curtiss, and K.J. Beers, *Rheol. Acta* **36**: 269 (1997).
- [4] H.C. Öttinger and F. Petrillo, *J. Rheol.* **40**: 857 (1996).
- [5] H. Tautz, *Exp. Tech. der Phys.*, **7**: 1 (1959).
- [6] D. Hands, *Rubber Chem. Tech.* **53**: 80 (1980).
- [7] B. Chitrangrad and J.J.C. Picot, *Poly. Eng. Sci.* **21**: 782 (1981); D.J. Wallace, C. Moreland and J.J.C. Picot, *Poly. Eng. Sci.* **25**: 70 (1985).
- [8] H. Janeschitz-Kriegl, *Polymer Melt Rheology and Flow Birefringence*, (Springer-Verlag, Berlin, 1983).
- [9] H. J. Eichler, P. Günter, and D. W. Pohl, *Laser-Induced Dynamic Gratings* (Springer, Berlin, 1986).
- [10] W. Köhler, C. Rosenauer and P. Rossmannith, *Int.J.Thermophys.* **16**: 11 (1995).
- [11] M. Okuda and A. Nagashima, *High Temp.-High Press.*, **21**: 205 (1989).
- [12] D.C. Venerus, J.D. Schieber, H. Iddir, J.D. Guzmán and A.W. Broerman, *J. Poly. Sci.: Poly. Phys. Ed.*, **37**: 1069 (1999).
- [13] D.C. Venerus, J.D. Schieber, H. Iddir, J.D. Guzmán and A.W. Broerman, *Phys. Rev. Lett.*, **82**, 366 (1999).
- [14] A.W. Broerman, D.C. Venerus and J.D. Schieber, *J. Chem Phys.*, **111**; 6965 (1999).
- [15] H. Miyamoto and A. Nagashima, *Int.J.Thermophys*, **17**: 1113 (1996).

Table 1. Summary of stress-optical and stress-thermal coefficients a 25°C.

Polymer	$D_{\text{eq}} \times 10^3$ [cm ² /s]	λ_{max}	$C \times 10^9$ [Pa ⁻¹]	$C_t \times 10^7$ [Pa ⁻¹]
poly-isobutylene melt	0.66 ± 0.03	6.1	2.0	1.6
cross-linked poly-siloxane	1.08 ± 0.02	2.1	0.17	1.3

FIGURE CAPTIONS

Figure 1. Photodetector voltage versus time following a step strain $\Upsilon = 8$ for poly-isobutylene melt. The origin of the time axis is 150 msec after the imposition of the strain. The symbols are the data and the solid line (decay only) is the fit of Eq. (7). The inset shows a histogram of the residuals along with a Gaussian distribution.

Figure 2. Dependence grating relaxation time τ_g on grating period Λ according to Eq. (6) for two values of time following a step strain ($\Upsilon = 8$) for poly-isobutylene melt with the grating in flow direction. Solid lines through circles correspond to a time of 0.15 secs and through the squares correspond to a time of 1.5 secs. The dashed line represents the result for a quiescent liquid.

Figure 3. Normalized thermal diffusivity in flow D_{11} (open) and neutral D_{33} (filled) directions versus time following the imposition of a step shear strain for a poly-isobutylene melt: $\Upsilon = 4$ (triangles) $\Upsilon = 8$ (circles).

Figure 4. Normalized difference in thermal diffusivity versus birefringence for a poly-isobutylene melt subject to step shear strains: $\Upsilon = 4$ (triangles) $\Upsilon = 8$ (circles).

Figure 5. Normalized thermal diffusivity in stretch D_{11} (squares) and contraction D_{33} (triangles) directions versus elongation ratio for a cross-linked poly-siloxane.

Figure 6. Normalized difference in thermal diffusivity versus tensile stress ($\sigma = \tau_{11} - \tau_{33}$) for a cross-linked poly-siloxane subject to uniaxial elongation.

Figure 1

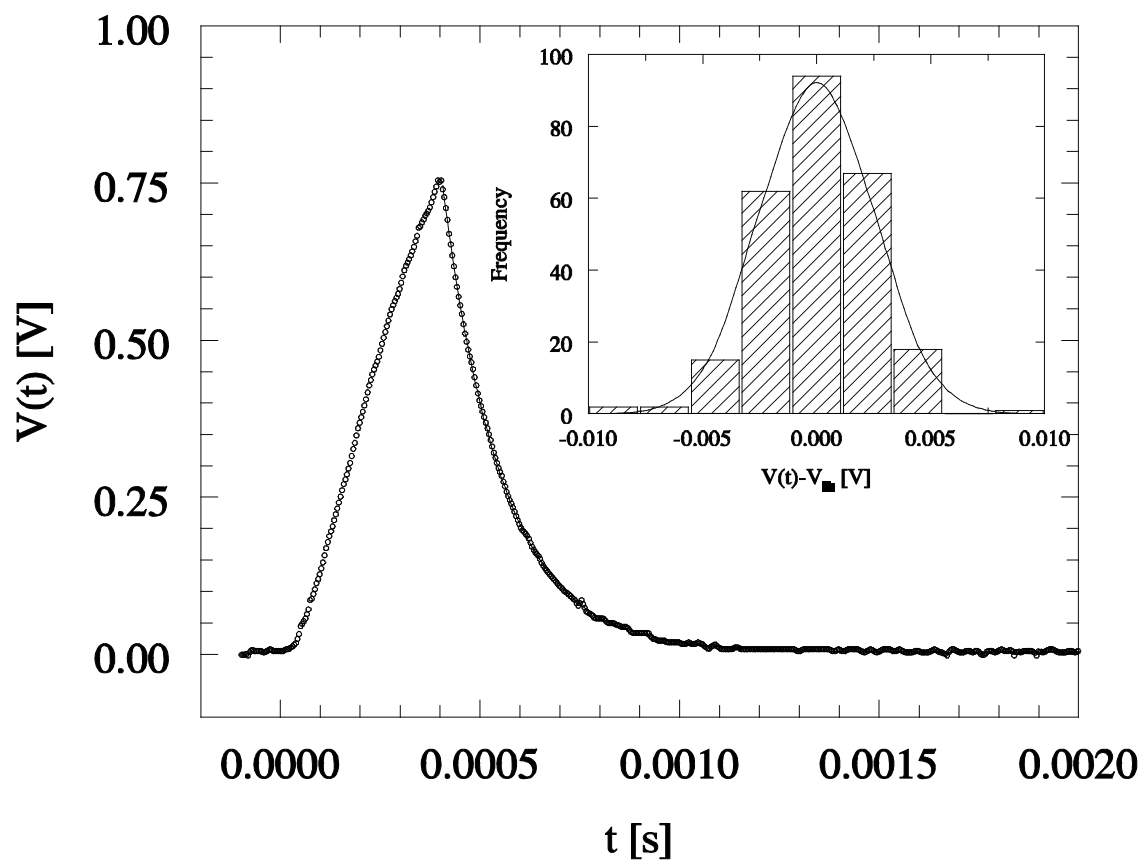


Figure 2

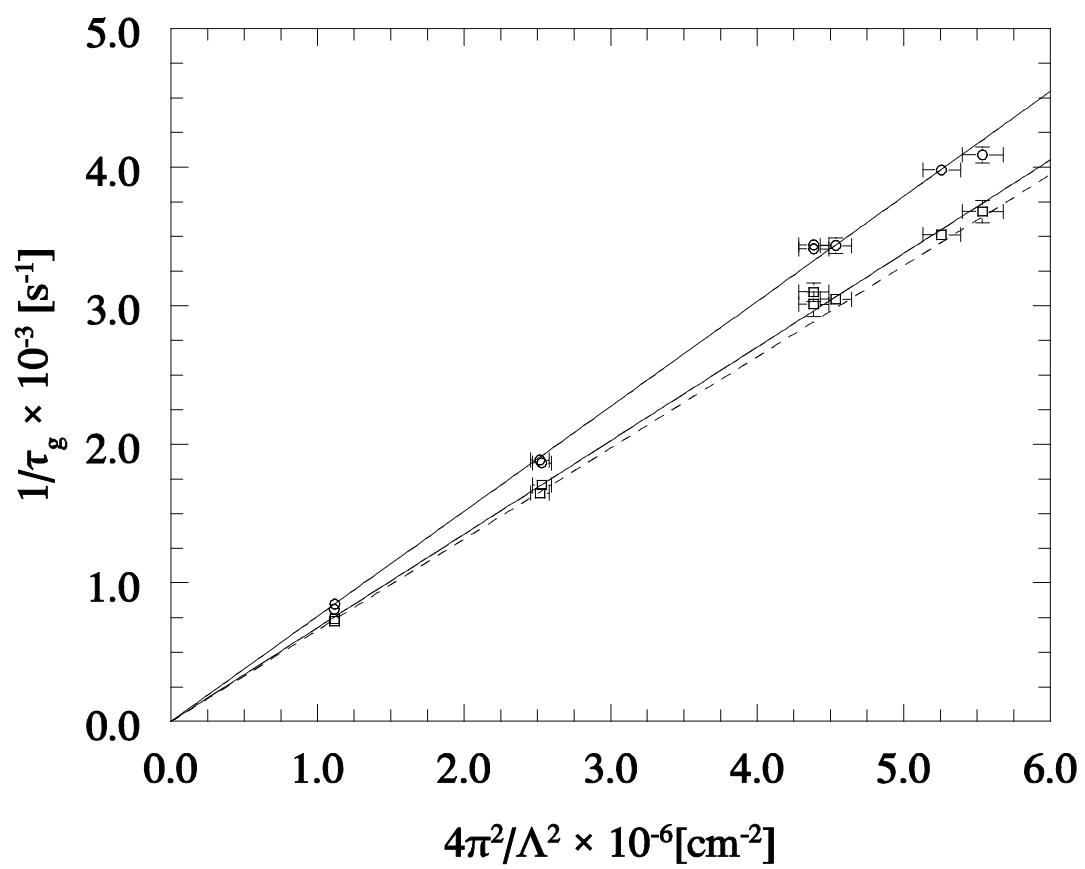


Figure 3

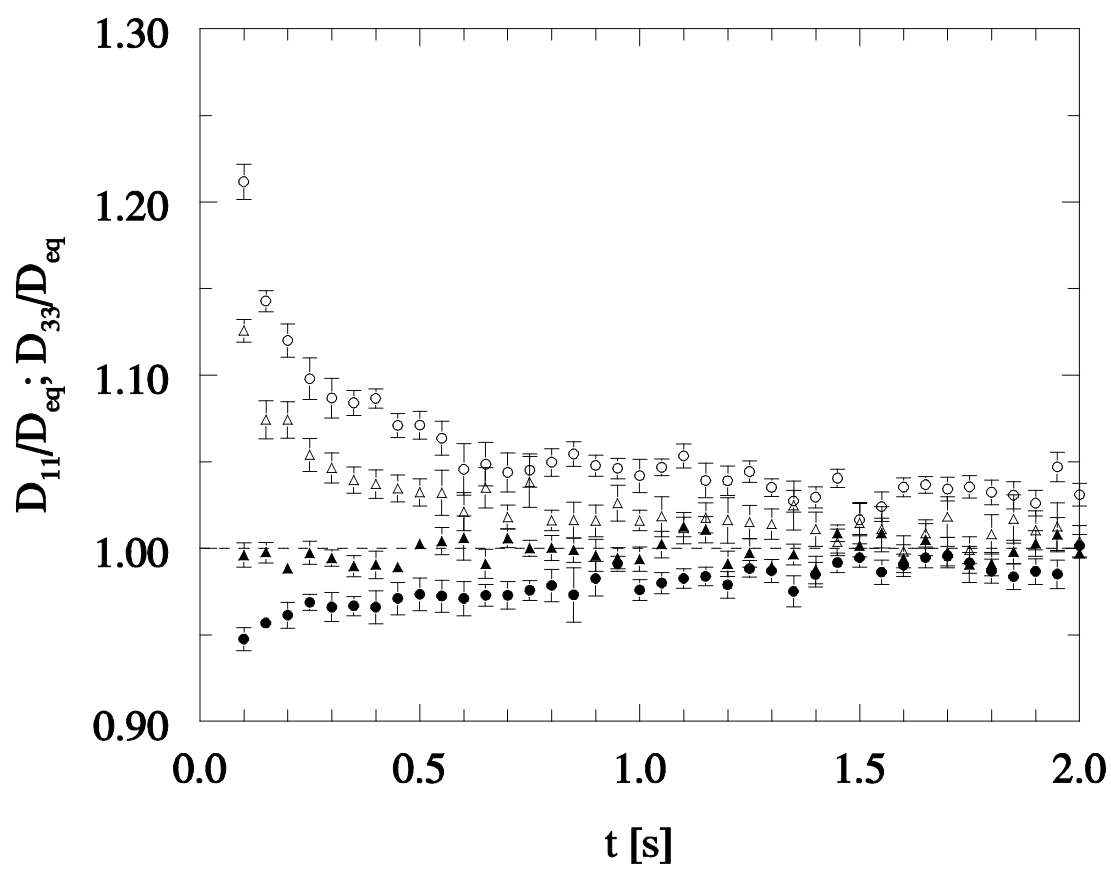


Figure 4

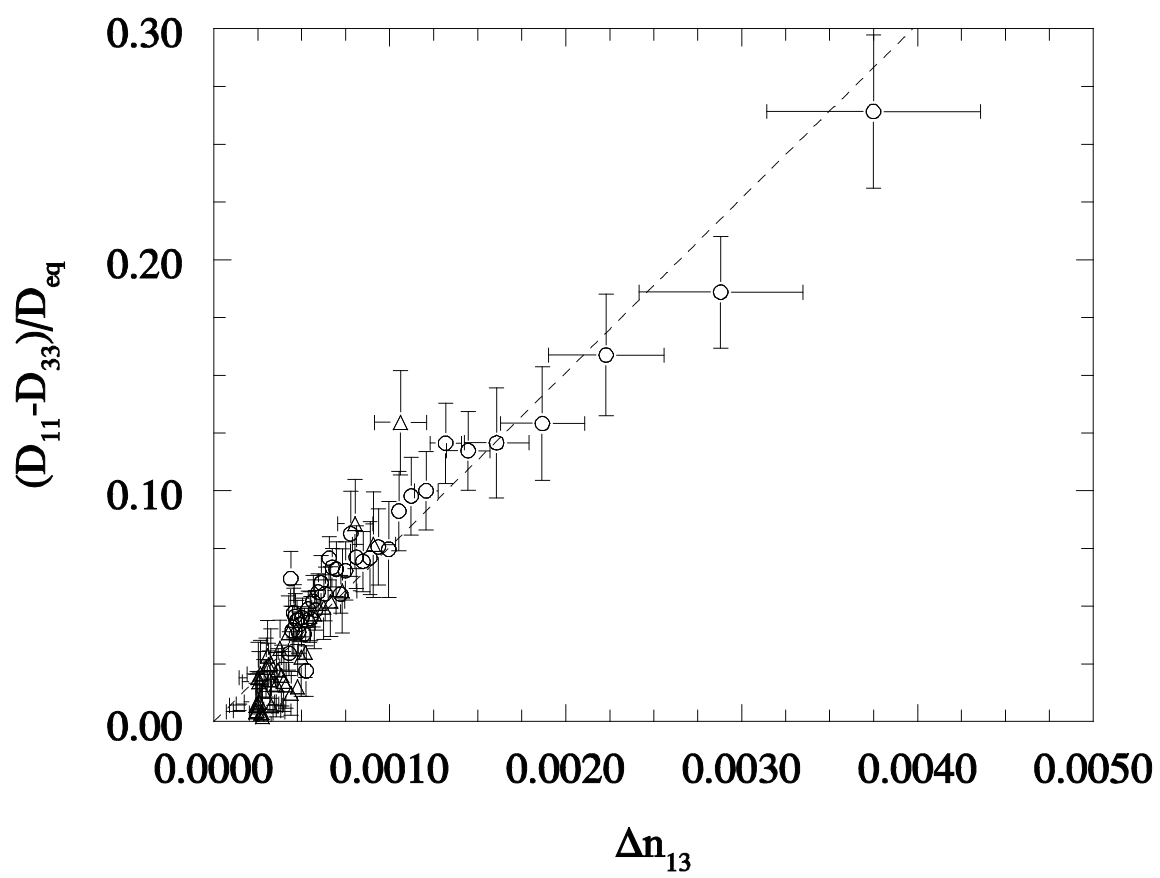


Figure 5

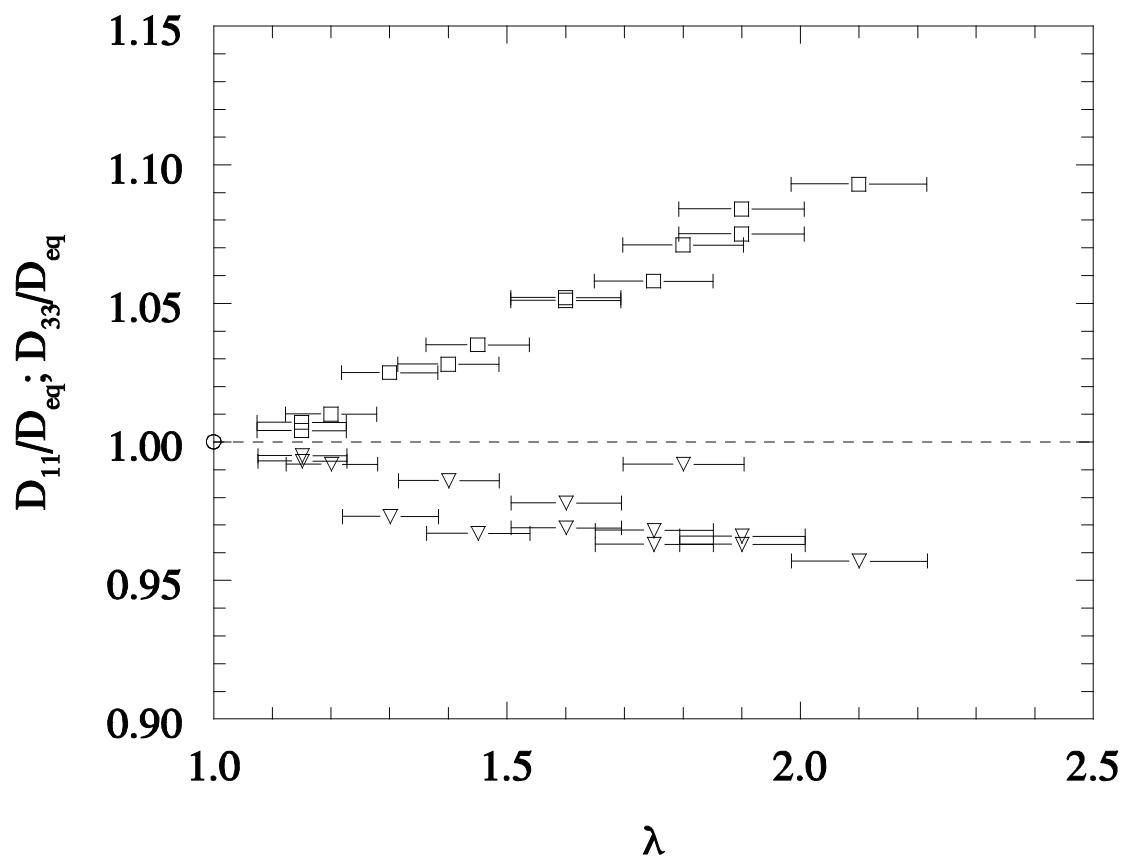


Figure 6

